INFLUENCE OF THE STORE ON THE TRANSONIC AND SUPERSONIC FLUTTER CHARACTERISTICS OF A DELTA WING CONFIGURATION

Hiroshi TERASHIMA*, Kozo FUJII**
***Intelligent Modeling Laboratory, The University of Tokyo**
****Japan Aerospace Exploration Agency**

Keywords: *delta wing with store flutter, store aerodynamics, CFD, transonic flow*

Abstract

Transonic flutter characteristics of a delta wing with external stores are simulated using the fluid/structure coupling method and the influence of the external store aerodynamics on the flutter characteristics are examined. Flow computations are carried out for the two-store configurations with different length and the effect of store configuration for the flutter characteristics is investigated. Existence of the external store influences on the pressure distributions of the lower surface of the wing especially in the supersonic flow region. The flutter boundary obtained for the wing with shorter store becomes different as that for the wing without store aerodynamics. On the other hand, the flutter boundary for the wing with longer store is generally similar to that for the wing without store aerodynamics. It is confirmed that the position of the shock wave over the lower surface of the wing is a key factor for the decision of the flutter boundary.

1 Introduction

The flutter has been a major aeroelastic problem for designing and cruising aircrafts. The aircrafts are given some fatal damage and then may be destroyed once the flutter occurs. Therefore, a number of experimental and numerical researches have been conducted over many years.

The flutter phenomena are influenced by some elements such as the Mach number, the external store/nacelle attached to the wing, the control surface, and so on. For example, the effect of the Mach number is known well as the transonic dip phenomenon, in which the flutter dynamic pressure decreases considerably at the transonic flow region. As can be seen from the example of the transonic dip phenomenon, considering the effects of these elements in the flutter analysis is important for capturing flutter characteristics accurately.

It is known that the addition of external store such as engines and fuel tanks to clean wings are one of the sensitive parameters for flutter phenomena. Flutter characteristics of clean wings are affected considerably by the natural vibration characteristics changed by the stores mounted under the lower surface of the wing and the store aerodynamics that change the flowfields around the wing and on the wing surface. In the experimental approach, Doggett and Ricketts [1] presented that an arrow wing with two nacelles has deeper transonic bucket than a clean wing. They also reported in their paper that the geometry of the nacelles has an effect on the flutter boundary. These results indicated that the difference in the flutter boundary is attributed to the difference in the nacelle aerodynamics because the natural vibration characteristics of the two nacelle configurations were essentially the same. Cole et al. [2] reported that the external store configuration has a significant effect on the transonic flutter boundary of a high-aspect-ratio wing. This result also shows the importance of the external store aerodynamics on the flutter characteristics as the two store configurations had the same mass and pitch and yaw inertia. Although these experimental results indicated

that the store/nacelle aerodynamics have influences on the flutter characteristics, the corresponding flowfields around the wing with external stores/nacelles behind the flutter characteristics have not been observed and discussed at all in the past experimental researches.

In the computational analysis, the store/nacelle aerodynamics is usually not included in the conventional flutter approaches as the effect of stores has been considered to be small and/or it is difficult to model the store aerodynamics simply especially in the transonic flow region. Although earlier numerical research [3] showed that the inclusion of external store aerodynamics was significant, it did not have discussion about the flowfields behind flutter characteristics like the experimental researches. Therefore, effects of external store aerodynamics on the flutter characteristics have not been clarified yet in both experimental and numerical approaches.

In our recent research [4] that applied the sophisticated Computational Fluid Dynamics (CFD) method for the estimation of external store aerodynamics, the influence of external store aerodynamics on the flutter boundary for a delta wing was investigated. The effect of number of stores was also investigated. The result showed that the store aerodynamics has a destabilizing effect in the supersonic flow region. The reason that the flutter dynamic pressure lowers by the store aerodynamics is in the location of the shock wave generated ahead of the external store on the lower surface of the wing. Since one store configuration was only considered in that study, it is worthwhile to simulate the flutter characteristics using different store configurations and sizes for the validation of the speculative conclusion.

The purpose of the present study is to reconfirm the reason for the reduction of the flutter dynamic pressure caused by the external store aerodynamics obtained in our previous research. For that purpose, longer store configuration is considered as a new store configuration and the effect of the external store aerodynamics on the flutter characteristics is examined in this study.

2 Numerical Procedure

2.1 Governing Equations and Methods for Aerodynamics

The governing equations for aerodynamics are the three-dimensional unsteady compressible Navier-Stokes equations written in the generalized coordinate system. The thin-layer approximation is used in this study. The convective terms are evaluated by the SHUS scheme [5], which is a family of AUSM-type schemes. The higher-order spatial accuracy is obtained by using the MUSCL with the primitive variable interpolation. The viscous term is discretized by the central differencing and the eddy viscosity is modeled by the Baldwin-Lomax turbulence model [6].

The time derivative is discretized by the three-point backward differencing with the inner-iteration algorithm [7], which could vanish the factorization and diagonalization error of the left hand side operator by the minor modification of the baseline solver. The LU-SGS implicit method [8] is used by the time integration. The present scheme can maintain the second-order temporal accuracy.

The ratio of the metrics and the Jacobians is taken to be the appropriate projected area of cell faces and the reciprocal of the Jacobians is taken to be the cell volumes. The metrics and the Jacobians obtained by such an approach satisfy the geometric conservation law for the moving and deformed grids [9].

At the inflow boundary, the freestream values are specified. At the subsonic outflow boundary, the pressure is fixed to the freestream value and other physical values are extrapolated. At the supersonic outflow boundary, all physical values are extrapolated. On the wall boundary, the density is extrapolated and the flow velocity matches to the wall velocity, which is equal to the grid speed. The normal momentum equation is accounted for the wall acceleration effect on the pressure gradient.

2.2 Governing Equations and Methods for Structural Dynamics

The linear equations of motion are used for the computation of the structural deformation under an aerodynamic force. The mass and the stiffness matrix used in the equations are derived using the finite element modeling. In this study, the governing equations can be solved using the modal approach, in which the solutions are composed with the eigenvectors of the free vibration problem. The resulting equations become as follows:

$$M_i \ddot{q}_i + M_i \omega_i^2 q_i = \{\phi_i\}\{f\}, \quad i = 1, \cdots, N \quad (1)$$

and

$$\omega_i^2 = \{\phi_i\}^T [K]\{\phi_i\}, \quad M_i = \{\phi_i\}^T [M]\{\phi_i\}$$

where q_i is the generalized displacement of the i-th mode and the vector $\{f\}$ of the right hand side represents the aerodynamic force obtained by solving the Navier-Stokes equations. ω_i, M_i, and $\{\phi_i\}$ are the natural frequency, the generalized mass, and the eigenvector of the i-th mode, respectively. N is the degree of freedom considered. Finally, the equations (1) can be rewritten the following first-order system by defining $S_i = \{q_i \quad \dot{q}_i\}^T$.

$$\dot{S}_i + \begin{bmatrix} 0 & -1 \\ \omega_i^2 & 0 \end{bmatrix} S_i = \begin{Bmatrix} 0 \\ \{\phi_i\}^T \{f\} / M_i \end{Bmatrix} \quad (2)$$

The time derivative operator in eqs. (2) is discretized by the three-point backward differencing with the inner-iteration under the same manner as that for the aerodynamic equations.

2.3 Coupling Procedure

The fully implicit coupling procedure proposed by Melville et al. [10] is adopted for removing the sequencing effect between the aerodynamic and the structural equations. This scheme is formed by coupling the aerodynamic equations with the structural equations through the inner-iteration. The second-order temporal accuracy can be maintained as a whole if the solution is converged through inner-iterations at each physical time step.

In this study, the structural grid points for the wing are mostly provided with a plate model neglecting any thickness effect but fluid grid points conform to the full geometry of the problem, in which case the fluid and the structural surface grid points do not actually lie on the same surface. Therefore, the information exchanges between the fluid and the structural grid points are required.

The Infinite Plate Spline (IPS) method [11] is used for the interpolation of the displacement from the structural grid points to the fluid grid points. Firstly, the fluid grid points are projected to the surface of the structural grid points. The deformations obtained at each structural grid point are interpolated on the projected fluid grid points by the IPS method. The new geometry can then be obtained by adding the thickness in the normal direction to the deformed fluid grid points.

The grid deformation approach developed by Melville et al. [10] is employed to generate a time varying fluid grid system between the wing surface and the far field. This algebraic method can maintain the grid quality of the initial grid near the deformed surface under arbitrary, moderate deflections and rotations.

The mapping algorithm presented by Bhardwaj et al. [12] is applied to transfer the aerodynamic forces from the fluid grid points to the structural grid points. The aerodynamic forces are calculated at each fluid grid point using the pressure, the shear stress, and the corresponding computational area. The aerodynamic forces are then mapped onto the structural grid points. Details of this algorithm can be found in Ref. [12].

2.4 Model Geometry

The geometric properties of the model configuration used in this study are shown in Fig. 1. These properties are essentially based on several experimental models [1,2,13]. In particular, the wing model is the same as that used in the experiment of Doggett et al. [13]. The wing model is a clipped delta wing with the

aspect ratio of 0.54 and the leading edge sweepback angle of 72 degrees. The modified biconvex airfoil section has a thickness of 0.03 based on each chord length. The wing model was constructed of a 0.051-inch-thick aluminum alloy plate that was covered by the balsa wood.

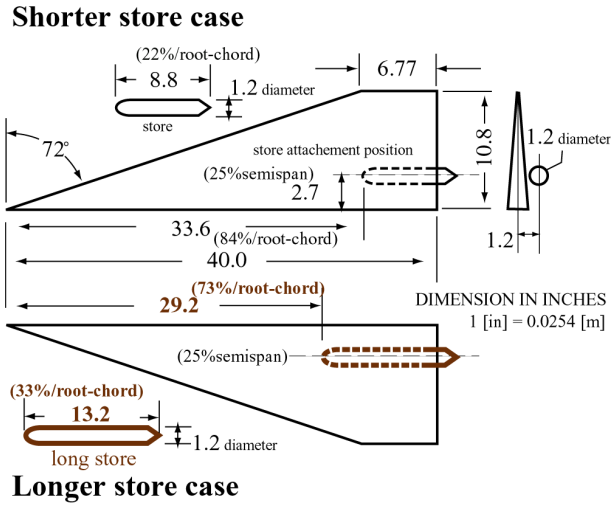

Fig. 1 Model geometry for the wing with two different store configurations.

The external store that simulate an engine nacelle or a fuel tank are rear-mounted on the under side of the wing at about 25 percents of the wing semispan as shown in Fig. 1. The location of the external store is determined for simulating the store location as seen well in typical high-speed aircraft configurations such as Concorde or future space planes. In this study, two different store configurations are considered and the effect of the store aerodynamics on flutter characteristics is examined. In Fig. 1, the first store configuration (indicated in Fig. 1 as shorter store case) is the same as that used in our past research [4] and the second one (indicated also in Fig. 1 as longer store case), which has the long length for the first store configuration is considered. The length of the second store is 1.5 times that of the first one. Although the length is different between two stores, it is assumed that the mass of each store becomes the same. Each store provides a concentrated mass of about one-half of the wing mass and is assumed to be made only by steel plates.

In the finite element structural analysis, it is modeled that the wing is consisted only of the aluminum alloy plate for simplicity. Due to this modeling, the weight of the wing becomes about 0.53 times lower than that used in the experiment of Doggett et al. [13] because the balsa wood, which covered the aluminum alloy plate is not considered. The mass ratio that is one of important parameter for flutter phenomena is varied by the decrease of the wing weight. In order to match the mass ratio to the experiment, the freestream density of the flow condition is corrected to be small in the computations. Influences by the decrease of the weight are also described at the following section.

2.5 Computational Fluid Grid

The overset grid approach is conducted for the delta wing with external store configuration. The Fortified solution algorithm proposed by Fujii [14] is applied to the information exchange between each grid. One example of the computational fluid grid used in this study is shown in Fig. 2. The computational grid for the delta wing is topologically C-H type, which has 273×65×61 grid points. The outer boundary is located at 30 times wing root-chord length away from the wing surface. The computational grid for the external store is topologically O-O type, which has 73×69×29 grid points. The total grid point is about 1.2 million.

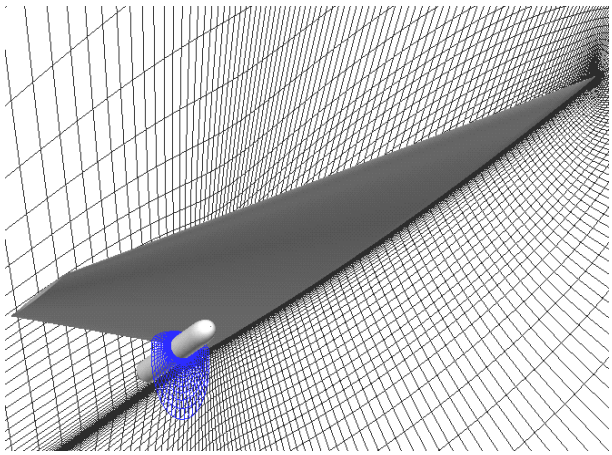

Fig. 2 Computational fluid grids.

2.6 Flow Condition

Flow conditions are taken directly from the transonic and supersonic delta wing flutter experiment conducted by Doggett et al. [13]. Freestream Mach number is set up from 0.85 to 1.22, and the corresponding Reynolds number based on the wing root-chord length becomes from 2.3×10^6 to 4.5×10^6. As described previously, the value of freesteam density is set to be smaller than that in the experiment.

2.7 Vibration Characteristics

The natural vibration frequencies and eigenvectors are first computed by solving the generalized eigenproblem arising from finite element discretizations. The delta wing, the external store, and the pylon are modeled using quadrilateral shell elements, respectively. A typical finite element model used in this study is shown in Fig. 3. The wing model is consisted of 484 elements. The external store and pylon is consisted of 76 elements.

In this study, although two different external stores are considered, it is assumed that they have the same vibration characteristics since the main purpose of this study is to investigate the effect of external store aerodynamics.

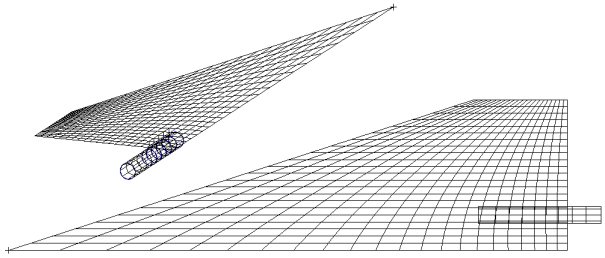

Fig. 3 Structural finite element model of the wing with external store.

The computed first three node lines and the corresponding natural frequencies for the clean wing and the wing with external store are presented in Figs. 4, respectively. The natural frequencies for the wing with external store are taken to be smaller values than that for the clean wing over all the modes due to the addition of the external store. In Figs. 4, each solid line drawn on the wing surface represents nodal lines, on which the magnitude of eigenvectors becomes to zero. As also seen in Figs. 4(a) and 4(b), the first mode corresponds to the primary bending mode, the second mode to the primary torsion mode, and the third mode to the second torsion mode, respectively. The nodal pattern for the wing with external store is generally similar to that for the clean wing except for the third mode.

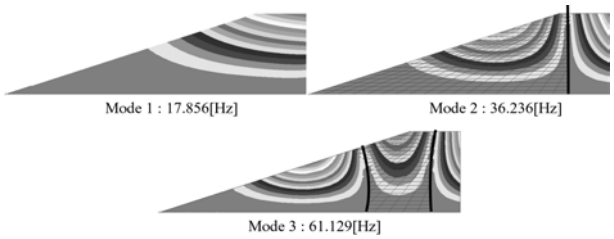

(a) clean wing

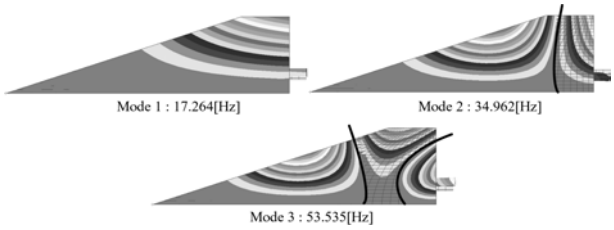

(b) wing with external store

Fig. 4 Comparison of the node lines and the natural frequencies for the first three modes.

2.8 Flutter Data Processing

The nondimensional time step size used in this study is taken to Δt=0.005. Preliminary numerical experiments show that the time step size, Δt=0.005 with three times inner-iterations is enough to estimate the time histories of wing displacement. All the computations start with the corresponding steady-flow results. The first seven vibration modes are considered and a small perturbation $\dot{q}_1 = 0.0001$ is given to the structural equations (2).

In order to determine the flutter boundary at a given Mach number, the time responses of the wing displacement are observed under several values of freestream dynamic pressure. In this study, the freestream velocity is varied according to the change of freestream dynamic pressure. The freestream density is fixed. The

change of freestream velocity leads to the change of Reynolds number.

3 Results and Discussions

3.1 Results of the shorter store

At first, the results obtained in our former research [4] are shown briefly below to make the discussions clear. Figures 5 shows the flutter dynamic pressure and the flutter frequency with Mach number obtained in the three cases, respectively.

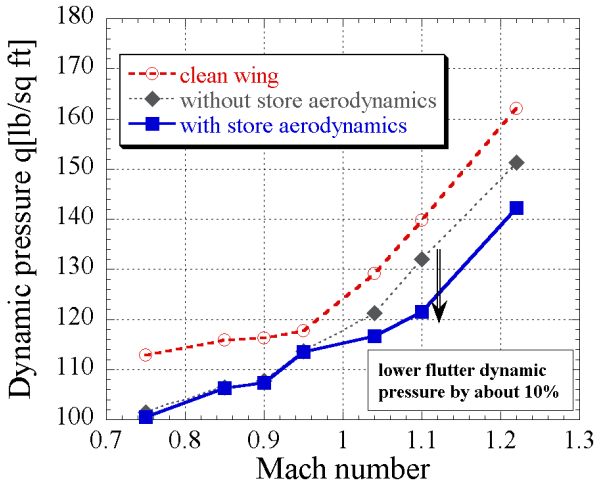

(a) Dynamic pressure

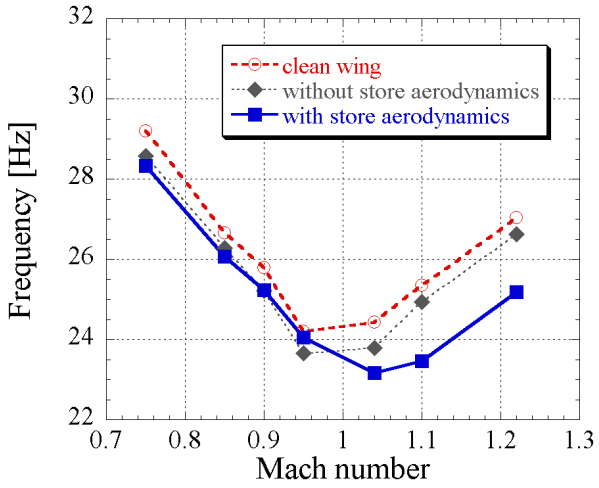

(a) Frequency

Fig. 5 Comparison of flutter boundaries for the three cases obtained in the former research.

The three cases plotted in Figs. 5 are as follows: (1) clean wing, (2) wing with store in structure and without store aerodynamics, (3) wing with store in structure and with store aerodynamics. Case (2) means that the effects of external store are included in the structural analysis, but not in the aerodynamic (CFD) analysis. Namely, although the changes of modal shape and natural frequency by addition of external store are considered, the flowfields around the wing and on the wing surface are not disturbed by the external store as the external store is not included in the aerodynamic (CFD) analysis. This case corresponds to the conventional flutter analysis, in which the effect of store aerodynamics is not included.

As shown in Fig. 5(a), it is found that the flutter dynamic pressure for Case (3), in which the effects of store aerodynamics are considered, lowers than that for Case (2) in the supersonic region. This result means that neglecting the store aerodynamics leads to overestimation of the flutter dynamic pressures. The reason that the flutter dynamic pressure decreases could be explained by the observation of flowfileds as shown in Figs. 6. It was concluded that the location of the shock wave generated ahead of the external store on the lower surface of the wing in the supersonic flow region is important factor for the reduction of the flutter dynamic pressure as indicated in Fig. 6(b).

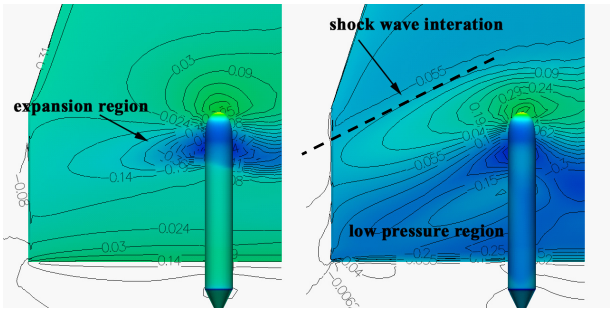

(a) M_∞=0.9 (b) M_∞=1.1

Fig. 6 C_p contour plots on the lower surface of the wing at two Mach numbers.

3.2 Results of the longer store

The wing with longer store is considered and the effect of the external store aerodynamics on the flutter characteristics is examined. The nose of the longer store is located more forward than that of the shorter store that was presented in Fig. 1.

Figures 7 (a)~(d) show the steady C_p contour plots over the lower surface of the wing at M_∞=0.85, 0.9, 1.1, and 1.22 respectively. Also included in Figs. 7 are the steady C_p contour plots obtained in the shorter store case to contrast the position of the shock wave. At M_∞=0.85 (Fig. 7 (a)), the effect of the external store on the lower surface of the wing is observed as the generation of expansion regions only at the shoulder of the external store for both the cases. At M_∞=0.90 (Fig. 7 (b)), the pressure distributions on the wing surface are influenced only near the external store although the expansion regions become larger than the M_∞=0.85 case. As the uniform flow reaches the supersonic velocity, the shock wave is generated ahead of the external store and interferes with the lower surface of the wing at both the cases as shown in Figs. 7 (c) and 7(d). The shock wave on the wing surface in the longer store case is located more forward than that observed in the shorter store. The shock wave for the longer store does not interfere with the tip regions of the wing unlike the shorter store. These steady-flow results obtained in the longer store case may indicate that the external store aerodynamics has little effect on the flutter characteristics though the pressure distributions over the lower surface of the wing are influenced by the shock wave as well as the shorter store case where the flutter dynamic pressure decreases.

Computed flutter characteristics for the shorter store case and the longer store case are shown in Figs. 8 (a) and 8(b). Also included in Figs. 8 is the flutter characteristic of the wing without store aerodynamics. Since it is assumed that the vibration characteristics of the two different store configurations are the same, the result for the wing without store aerodynamics can be compared with both the store cases. The plots of the wing without store aerodynamics and the wing with the shorter store are the same as presented in Figs. 5.

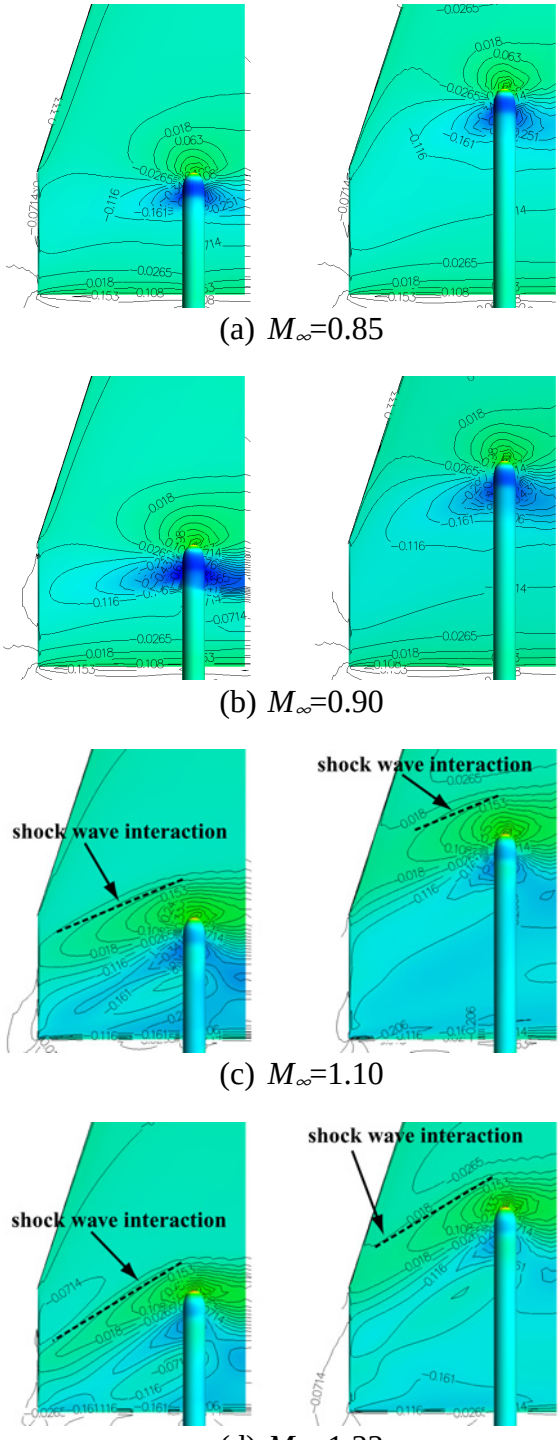

(a) M_∞=0.85

(b) M_∞=0.90

(c) M_∞=1.10

(d) M_∞=1.22

Fig. 7 C_p contour plots over the lower surface of the wing for the wing with shorter store (left) and longer store (right).

In Fig. 8 (a), the flutter dynamic pressures for the wing with longer store take the similar values with those for the wing without store aerodynamics at all the Mach numbers unlike the shorter store case. This trend can be also confirmed from the results of the flutter frequencies as seen in Fig. 8 (b). Figure 9 shows the time responses of the first mode obtained by each store cases at the same flow condition. The time response for the longer store case tends to converge with the time although the time response for the shorter store case grows due to the influence of the store aerodynamics. These results indicate that it is not necessarily required to include the store aerodynamics in the wing-store flutter analysis even when the shock wave ahead of the external store interferes strongly with the lower surface of the wing.

In the longer store case, the external store aerodynamics has little effects on the flutter characteristics although it influences the flow fields over the lower surface of the wing. Since the strength of the shock wave generated ahead of the external store is almost the same for both the cases, the results obtained in this study also indicate that the position of the shock wave becomes important on the decision of the wing-store flutter boundary as described in the former research.

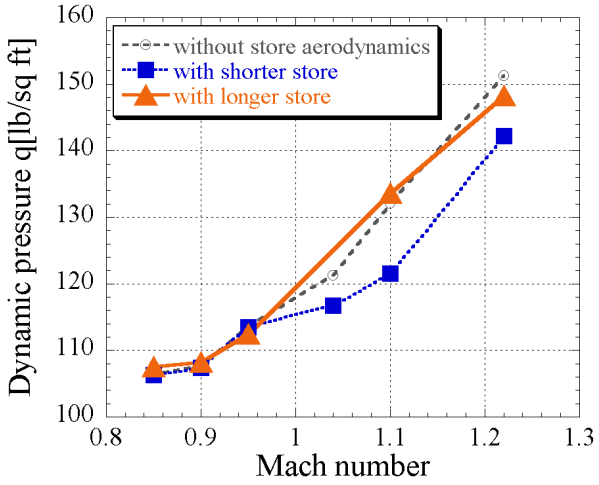

(a) Dynamic pressure

Fig. 8 continued.

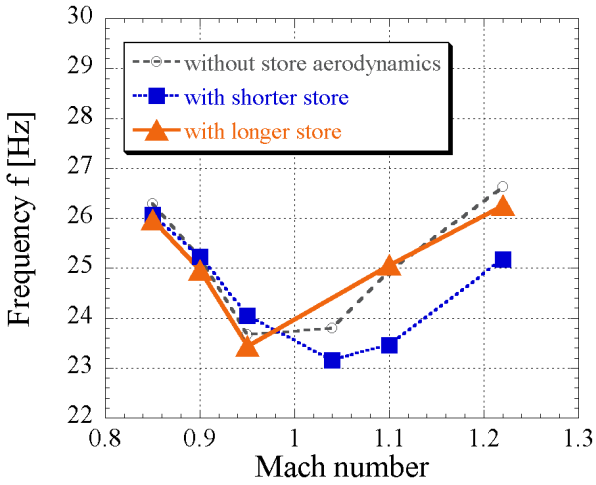

(b) Frequency

Fig. 8 Flutter boundaries for the two different store configurations and for the wing without store aerodynamics.

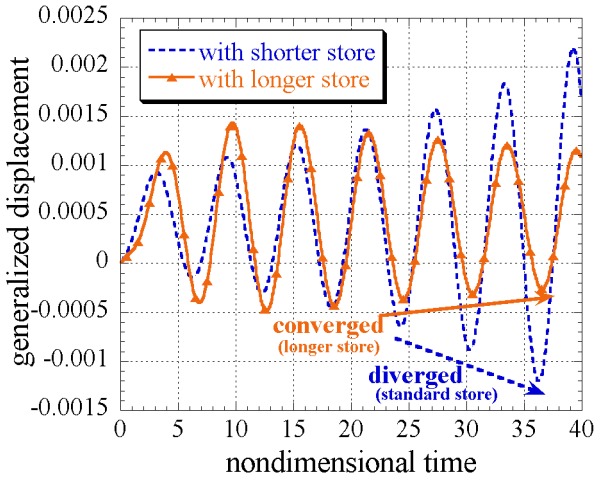

Fig. 9 Time responses of the first mode for the two different store configurations at the same flow condition.

4 Conclusion

The influences of the external store aerodynamics on the transonic and supersonic flutter characteristics of the simple delta wing are numerically investigated by the computational simulation of the flows over the wing with two different external store configurations. Although the longer store has strong influence on the pressure distributions of the lower surface of the wing especially in the supersonic flow, the resulting flutter

characteristics are generally similar to that obtained by the case of the wing without store aerodynamics. The reduction of the flutter dynamic pressure caused by the inclusion of the external store aerodynamics was not observed in the longer store case. These results showed that the position of the shock wave generated ahead of the external store on the lower surface of the wing is important for the transonic and supersonic wing-store flutter characteristics. They also justified the estimation that the reduction of the flutter dynamic pressure is caused by the external store aerodynamics as described in our former research.

References

[1] Doggett R. V. Jr, Ricketts R. H. Some experimental and theoretical flutter characteristics of an arrow-wing configuration, AIAA Paper 77-422, 1977.

[2] Cole S. R, Jose A. R. and Nagaraja K. H. Flutter study of an advanced composite wing with external stores, AIAA Paper 87-0880, 1987.

[3] Turner C. D. Effect of store aerodynamics on wing/store flutter. *AIAA Journal*, Vol. 19, No. 7, pp 1121-1129, 1981.

[4] Terashima H and Fujii K. Effects of number of stores on the transonic flutter characteristics of a delta wing configuration, AIAA Paper 2004-2234, 2004.

[5] Shima E and Jounouchi, T. Role of CFD in aeronautical engineering (No. 14) – AUSM type upwind schemes, *Proceedings of the 14th NAL Symposium on Aircraft Computational Aerodynamics*, Japan, SP-34, pp 7-12, 1997.

[6] Baldwin B. S and Lomax, H. Thin layer approximation and algebraic model for separated turbulent flows, AIAA paper 78-257, 1978.

[7] Chacraverthy S. R. Relaxation methods for unfactored implicit upwind schemes, AIAA Paper 84-0165, 1984.

[8] Yoon S and Jameson A. Lower-upper symetric-gauss-seidel method for the euler and navier-stokes equations. *AIAA Journal*, Vol. 26, No. 9, pp 1025-1026, 1988.

[9] Tamura Y and Fujii, K. Conservation law for moving and transformed grids, AIAA Paper 93-3365-CP, 1993.

[10] Melville R. B, Morton S. A and Rizzetta D. P. Implementation of a Fully-implicit, aeroelastic navier-stokes solver, AIAA Paper 97-2039, 1997.

[11] Harder R. L and Desmarais R. N. Interpolation using surface splines. *Journal of Aircraft*, Vol. 9, pp 189-191, 1972.

[12] Bhardwaj M. K, Kapania R. K, Eichenbach E and Guruswamy G. P. Computational fluid dynamics/computational structural dynamics interaction methodology for aircraft wings. *AIAA Journal*, Vol. 36, No. 12, pp 2179-2186, 1998.

[13] Doggett R. V. Jr, Soistmann D. L, Spain C. V, Parker E. C and Silva W. A. Experimental transonic flutter characteristics of two 72°-sweep delta-wing models, NASA TM 101659, 1989.

[14] Fujii K. Unified zonal method based on the fortified solution algorithm. *Journal of Computational Physics*, Vol. 118, pp 92-108, 1995.